

HIGH PRESSURE PHASE BEHAVIOUR OF THE SYSTEM R23 + PHENYLPROPANE. EXPERIMENTAL RESULTS AND MODELING LIQUID-VAPOUR EQUILIBRIUM

Cristina BOGATU,^{*a} Rodica VÎLCU,^b Dan GEANĂ,^c Anca DUȚĂ,^a Wim POOT,^d
and Theodor W. de LOOS^d

^aTransilvania University of Braşov, The Centre Product Design for Sustainable Energy, Iuliu Maniu 50, 500091 Braşov, Roumania

^bUniversity of Bucharest, Faculty of Chemistry, Chemical-Physics Dept., M. Kogălniceanu Bd. 36-46, Sector 5, 70709 Bucharest, Roumania

^cPolitehnica University of Bucharest, Faculty of Applied Chemistry and Materials Science, Applied Physical Chemistry and Electrochemistry Dept., Calea Griviței 132, Sector 1, 011061 Bucharest, Roumania

^dDelft University of Technology, Mech., Process and Energy Dept., Laboratory for Engineering Thermodynamic Leeghwaterstraat 44, 2628CA Delft, The Netherlands

Received September 4, 2008

Equilibrium data for asymmetric systems consisting of refrigerant, R23 and 1-phenyl propane at temperatures $T=250-400$ K and pressures $P=1.5-15$ MPa are presented. The experiments were carried out in the Cailletet apparatus according to the synthetic methods. The investigated system exhibits type III phase behavior according to the classification of van Konynenburg and Scott.

PR and SRK EoSs coupled with 1PCMR and 2PCMR mixing rules were used for calculations of the LV equilibrium points. The predictive capabilities of the two EoSs were compared in terms of AADP.

INTRODUCTION

Mixtures consisting of refrigerant and lubricant oil are used as working fluids in the refrigeration and air conditioning systems. The lubricating agent is necessary for the correct functioning of the compressor, insuring the lubrication of the mechanical moving elements and the protection against the wear.¹

The presence of the lubricant oil in the refrigeration cycle influences the thermodynamic equilibrium and induces changes in the refrigerant composition and in the thermophysical properties of the refrigerants (LV equilibrium, enthalpy, viscosity, surface tension). The compatibility of refrigerant with lubricant must be discussed considering the phase equilibrium (liquid-vapour, liquid-liquid equilibria) that occurs during the system functioning. Based on these data, information on refrigerant solubility can be obtained. This is directly related to other properties of the refrigerant-lubricants mixtures such as: viscosity, lubricity. For these reasons, different models to describe the refrigerant - oil mixture have

been proposed in the literature.²⁻⁵ Many of them are based on equations of state (EoSs). They represent an important and useful tool to describe the thermodynamic properties and phase equilibrium of pure and fluid mixtures.

Nowadays, refrigerants from the hydrofluorocarbons (HFC's) represent an alternative to the classical chlorine containing compounds, which have been banned (Montreal Protocol), due to their environmental impact (ozone layer depletion and global warming effects). These refrigerants are used with synthetic lubricants like: alkylbenzenes for special applications at very low temperatures. However, alkylbenzenes cannot compete with other synthetic oil (polyol ester or polyalkylene glycol, poly- α -olefin, polyvinylether) because of their limited miscibility with the HFC compounds. Still, they present good chemical stability, low hygroscopic character and higher solubility in HFC's compared with aliphatic-based mineral lubricants.^{6,7}

This paper presents the experimental data on liquid-vapour (LV), liquid-liquid (LL) and liquid-liquid-vapour (LLV) equilibria for the asymmetric,

* Corresponding author: c.iosif@unitbv.ro

highly non-ideal system consisting of a HFC refrigerants-trifluoromethane (CHF_3 , R23) and alkylbenzene oil: 1-phenylpropane (phC3). According to the general classification of van Konynenburg and Scott, the system can develop type II, III, IV or V phase behavior. Two equations of state: Peng Robinson (PR) and Soave Redlich Kwong (SRK) coupled with one (1PCMR) or two parameters (2PCMR) van der Waals mixing rules were applied for the calculations of the LV equilibrium curves. The predictive capacity of the EoSs and the correlation of the parameters in the

mixing rules and the components structure are discussed.

EXPERIMENTAL

Chemicals

The trifluoromethane (CHF_3 , R-23) used was obtained from Praxair with a minimum purity of 99.995 %. The 1-phenylpropane (phC3) used was from Fluka, with a purity of 99.8 %. The chemicals were used without further purification. Some properties of these compounds are given in Table 1.

Table 1

Chemicals used and some properties

Name	Formula	T_b /K	T_m /K	T_c /K	P_c /MPa	ω^*
trifluoromethane	CHF_3	191.7 ^a	117.97 ^a	299.3 ^a	4.858 ^a	0.260 ^c
1-phenyl-propane	$\text{C}_6\text{H}_5\text{-C}_3\text{H}_7$	432.35	173.65	638.28 ^b	3.16b	0.344 ^c

a - calculated with Allprops

b - according to Nikitin *et al.*⁸

c-⁹

* ω - acentric factor

Procedure of measurements

The measurements were carried out with the so-called Cailletet apparatus described earlier by De Loos *et al.* (1983, 1986).¹⁰ Pressures up to 15 MPa can be applied and the temperature can vary from 250 K to 510 K.

A sample of the mixture with a known overall composition is confined over mercury in the top end of a narrow glass tube (Cailletet tube). The mixture is prepared by dosing the low-volatile compound (liquid at the room temperature) in the sealed end of the Cailletet tube by means of a micrometer syringe. The exact mass of the liquid component is determined by weighting. After the liquid is degassed, the gaseous component (light component) is added volumetrically using a mercury displacement method. The tube is mounted in a thermostat with circulating ethanol, water or silicon oil depending on the temperature range of interest. The temperature of the thermostat liquid is kept at the desired value with an accuracy better of than 0.02 K at temperatures up to 370 K.

The measurements consist of visually observation of the phase transitions when the pressure is slowly changed at constant temperature, or the temperature is slowly varied at constant pressure.

The pressure is measured with a dead-weight pressure gauge (type De Wit, accuracy of ± 0.003 MPa), or in the case of the measurements of liquid-liquid-vapour equilibrium with a manometer (Heise, uncertainty ± 0.01 MPa). The manometer was calibrated against the dead weight gauge.

A platinum resistance thermometer (Pt 100), previously calibrated against a standard thermometer, records the temperature of thermostat liquid near the sample with an accuracy of ± 0.01 K.

RESULTS AND DISCUSSION

a) Experimental results

Liquid-liquid-vapour equilibria (LLVE), liquid-vapour equilibria (LVE), liquid-liquid equilibria

(LLE) and the corresponding critical endpoint were measured for compositions range from 0.15 to 0.97 mole fraction of trifluoromethane (x), pressures $P = 1\text{-}15$ MPa and temperatures $T = 250\text{-}370$ K.

In Fig. 1 and Fig. 2 there are presented the bubble point curves together with the vapour pressure data for trifluoromethane and respectively the liquid-liquid phase boundaries.

The experimental data on vapour pressure and critical point for trifluoromethane ($T_c = 298.95 \pm 0.02$ K, $P_c = 4.79 \pm 0.005$ MPa), measured in this work agrees within the experimental uncertainty with the data reported elsewhere.^{11, 12}

The liquid-liquid-vapour curve (LLV) ends in an upper critical endpoint (UCEP – $L_2+L_1=V$) and goes uninterrupted to low temperatures. This indicates type III phase behaviour according to the general classification of Van Konynenburg and Scott. At the UCEP, the liquid L_1 , richer in the more volatile component – CHF_3 and the vapour phase merge in one single fluid phase. This critical fluid coexists with the second liquid phase, L_2 , richer in the less volatile component (the heavy component) – phC3.^{13, 15}

The coordinates of the UCEP were found at: $T = 312.24$ K, $P = 5.825$ MPa. For the studied system there are no data reported in the literature, so far.

Phase transition measurements (Fig. 1 and Fig. 2) show for samples with low composition in trifluoromethane, $x(\text{CHF}_3) = 0.1746 \dots 0.5047$, only bubble points, while for samples with higher content of CHF_3 ($x(\text{CHF}_3) = 0.5738 \dots 0.5505$), liquid split occurs. The LL and LV for every

composition meets in a point of the three-phase equilibrium line (LLV). The LL isopleths are steep curves in P-T diagrams, and moves to higher temperature and pressure when the mole fraction of CHF_3 increases. Thus, starting with composition of 0.5918 mole fraction of CHF_3 , the LV and LL lines join in one continuous curve, positioned above the three-phase equilibrium line, showing a pressure minim. The same trend will have the experimentally isopleths for mixtures with $x(\text{CHF}_3)=0.5918\dots 0.7991$. Particularly interesting is the isopleth for $x(\text{CHF}_3)=0.7991$, the maximum measured for the studied system. This value corresponds to the critical composition and, respectively the measured LL phase boundary represents the LL critical line. No, LL equilibrium

was experimentally observed at higher pressure and temperature. The samples with $x(\text{CHF}_3)$ values nearby to the critical composition ($x(\text{CHF}_3)=0.7028\dots 0.7622$ and respectively $x(\text{CHF}_3)> 0.7991$) are positioned under the critical LL curve. These isopleths moves slowly to lower pressures with increasing of the mole fraction of CHF_3 , and finally intersects the three-phase equilibrium line at $x(\text{CHF}_3)=0.9255$. Thus, mixtures with very low composition of ph-C3 (high $x(\text{CHF}_3)$), presents discontinuous LL curve: the first branch originates in the LLV three phase line at low temperature ($T=260\text{K}$) and goes very steep to higher pressure; the second is located in the region of higher temperatures and ends in the three phase line (around $T=298\text{K}$).

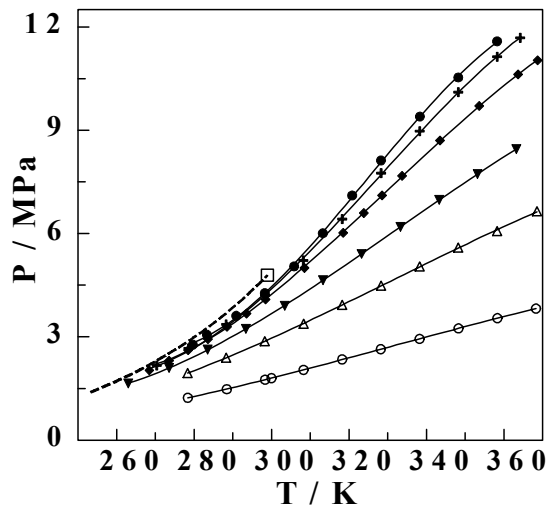


Fig. 1 – VLE in the system $x \text{CHF}_3 + (1-x) \text{phC}_3$: vapour pressure curve for CHF_3 (---), critical point of CHF_3 (□), bubble points curves for: $x=0.5738$ (●), $x=0.5541$ (+), $x=0.5047$ (◆), $x=0.4000$ (▼), $x=0.3006$ (△), $x=0.1746$ (○).

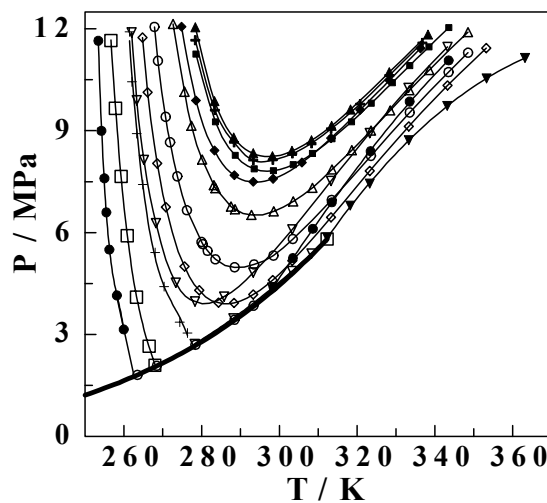


Fig. 2 – LL equilibria in the system $x \text{CHF}_3 + (1-x) \text{phC}_3$ for: $x=0.9605$ (▼), $x=0.9255$ (●), $x=0.8996$ (∇), $x=0.8502$ (◆), $x=0.8256$ (+), $x=0.7991$ (▲), $x=0.7028$ (■), $x=0.6510$ (△), $x=0.6101$ (○), $x=0.5918$ (◇), $x=0.5738$ (+), $x=0.5505$ (□); LLV equilibria (—), UCEP-upper critical endpoint, $L_2+L_1=V$ (□).

For the sample with $x(\text{CHF}_3) = 0.9605$, only the higher temperature branch could be measured. The second one is located at very low temperatures, out of the measurements range with the Cailletet apparatus.

Between the two LL branches, LV equilibrium points were experimentally observed. These are positioned slightly above (less than 0.04 MPa at fixed T) the three-phase LLV equilibrium line. That means the L_1V region is very narrow, confirmed also by the P-x cross-sections (Fig. 3, Fig. 4). The cross-sections were obtained by interpolation from the P-T diagrams. Three order polynomials were used to fit the experimental points. The maximum value of the residual was in the average or less than the error in the pressure measurements. In the isothermal P-x cross-sections, the L_2V region is separated from the upper two-phase regions: L_1L_2 and L_1V (very narrow) by means of the three-phase line. The isotherms change the character from LV curve to LL curve and show at approximately $x(\text{CHF}_3) = 0.7991$, a point of inflection corresponding to the critical composition. At the temperature of the UCEP and above L_1V region disappears and the two regions L_1L_2 and L_2V join in one single LV region, showing a horizontal point of inflection.¹³⁻¹⁶

b) Modelling

Calculations of the VLE data were done using two equations of state: PR and SRK EOSs for temperatures below and above the UCEP. These equations have been widely used and literature reports satisfactory results when applied in asymmetric mixtures, similar with the studied system.^{16, 17} The two EoSs are described by the relations (1) and (2), respectively. These are two parameters equations: a – measure of the attractive forces between the molecules and b – the co-volume occupied by the molecules (considering molecules as hard spheres).

$$P = \frac{RT}{v-b} - \frac{a(T)}{v(v+b) + b(v-b)} \quad (1)$$

where:

$$a = 0.45724 \frac{R^2 T_C^2}{P_C} \alpha(T)$$

$$\alpha(T_R, \omega) = [1 + m_{PR} (1 - T_R^{0.5})]^2$$

$$m_{PR} = 0.37464 - 1.54226\omega - 0.26992\omega^2$$

$$b = 0.077796 \frac{RT_C}{P_C}$$

$$P = \frac{RT}{v-b} - \frac{a(T)}{v(v+b)} \quad (2)$$

where:

$$a = 0.42748 \frac{R^2 T_C^2}{P_C} \alpha(T)$$

$$\alpha(T_{R,\omega}) = [1 + m_{SRK} (1 - T_R^{0.5})]^2$$

$$m_{SRK} = 0.480 + 1.574\omega - 0.176\omega^2$$

$$b = 0.08664 \frac{RT_C}{P_C}$$

To describe the interactions between the mixture components, van der Waals conventional mixing rules with one (1PCMR), respectively two parameters (2PCMR) were applied (relations (3, 4) and (5, 6)). The interactions parameters are k_{ij} for 1PCMR and respectively k_{ij} and h_{ij} for 2PCMR. They result from regression of the liquid-vapour equilibrium data for mixture.^{18, 19}

1 PCMR mixing rules:

$$a = \sum_i \sum_j x_i x_j a_{ij} \quad (3)$$

$$b = \sum_i x_i b_i \quad (4)$$

where:

$$a_{ij} = \sqrt{a_i \cdot a_j} (1 - k_{ij})$$

2 PCMR mixing rules:

$$a = \sum_i \sum_j x_i x_j a_{ij} \quad (5)$$

$$b = \sum_i \sum_j x_i x_j b_{ij} \quad (6)$$

where:

$$a_{ij} = \sqrt{a_i \cdot a_j} (1 - k_{ij})$$

$$b_{ij} = \frac{b_i + b_j}{2} (1 - h_{ij})$$

Considering the model described before, the VLE data for the system of CHF_3 + 1-phenylpropane were fitted. In Fig. 3 and Fig. 4 the isothermal P-x experimental data together with the calculated points using PR and respectively SRK EoSs are plotted. The interaction parameters in the mixing rules (2PCMR) obtained by bubble P optimization are given in Table 2.

The calculations using 1PCMR in the EoS, lead to unsatisfactory correlations for the entire range of temperatures, compared with the application of the

2PCMR. The average absolute deviation in pressure (AADP) is about 7-10%.

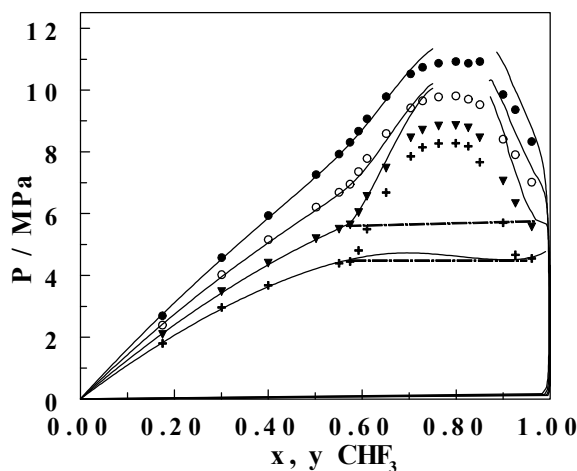


Fig. 3 – Isothermal P-x cross-sections for system $x \text{ CHF}_3 + (1-x) \text{ phC}_3$: 330 K(●);320 K(○); 310 K (▼); 300 K (+); PR/ 2PCMR (—), LLV line, this work (---).

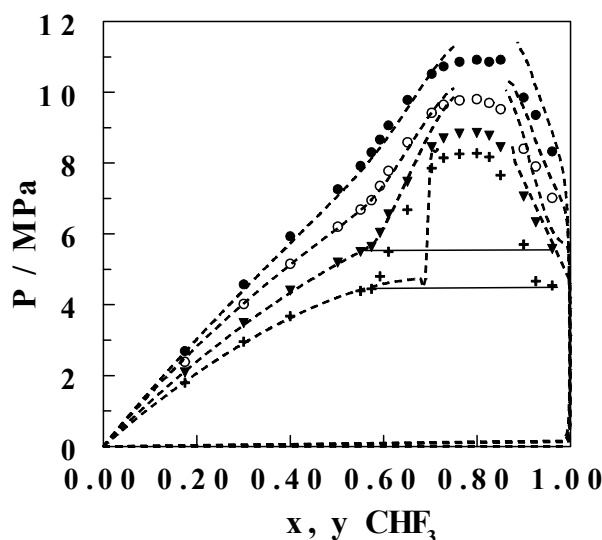


Fig. 4 – Isothermal P-x cross-sections for system $x \text{ CHF}_3 + (1-x) \text{ phC}_3$: 330 K(●);320 K(○); 310 K (▼); 300 K (+); SRK/2PCMR (---), LLV line, this work (- ·-).

The interaction parameter, k_{ij} obtained by regression with 1PCMR was further used as initial value in the 2 PCMR calculations. Thus, the model using both EoSs gives good description of the phase boundaries. This fact is confirmed once by the values of $\text{AADP} < 2\%$ (Table 2), and also by the distribution of the relative deviation in pressure ($\Delta P/P_{\text{exp}}$, $\Delta P = (P_{\text{cal}} - P_{\text{exp}})$) which has values very close to 0 for all the experimental points, Fig. 5.

The model (using both EoSs) fails in the region of LL separation and respectively in the critical region (Fig. 3 and Fig.4), the deviation in pressure being

quite pronounced (Fig. 5). This fact is characteristic to the asymmetric systems containing components with large differences in the size of molecules.¹⁶⁻²¹

Still, SRK EoSs is able to describe the phase behaviour at low temperatures, better representing the shape of the isotherm below the temperature of the UCEP, while PR EoSs shows good correlations capabilities at higher temperatures. The models fitting, based on both EoSs show under prediction at higher temperatures except the critical region, where over prediction is visible (model nonconvergence region).

Table 2

The interaction parameters calculated with PR and SRK EoSs for system x CHF₃ + (1-x) phC3

T[K]	Type of EoS	Parameters		AADP [%]
		k ₁₂	h ₁₂	
300	PR	0.0843	-0.0318	1.11
	SRK	0.0831	-0.0313	1.16
310	PR	0.0829	-0.0337	0.96
	SRK	0.0825	-0.0329	0.94
320	PR	0.0792	-0.037	1.58
	SRK	0.079	-0.0392	1.38
330	PR	0.0781	-0.0394	1.21
	SRK	0.0798	-0.0337	2.21

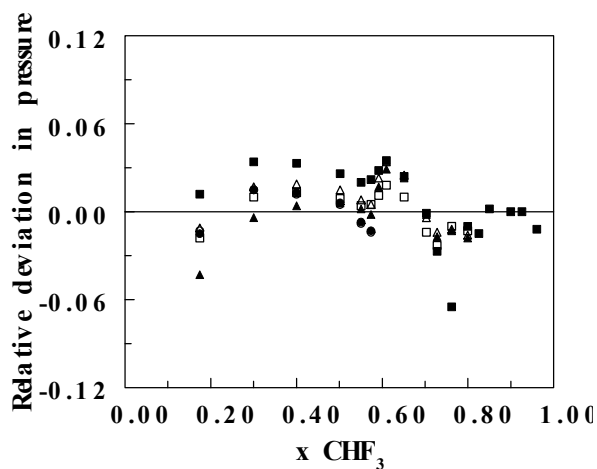


Fig. 5 – Relative deviation in pressure ($\Delta P/P_{\text{exp}} = (P_{\text{cal}} - P_{\text{exp}})/P_{\text{exp}}$) for system x CHF₃ + (1-x) phC3: 300 K/ SRK(●); 300 K/ PR(○); 320 K/ PR(▲); 320 K/ PR(△); 330K/ SRK (■); 330K/ PR(□).

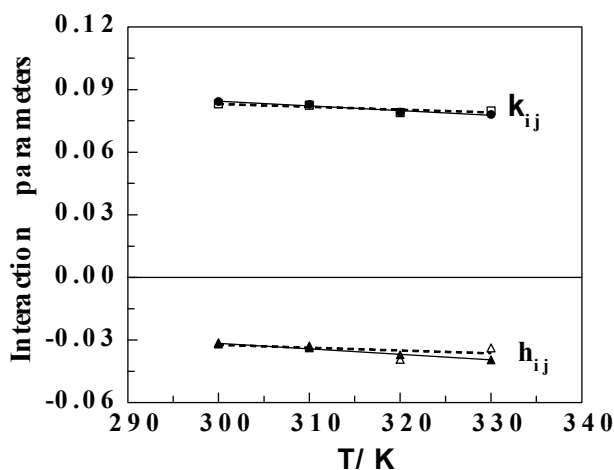


Fig. 6 – Variation of the interactions parameters with temperature: PR (—); SRK (---).

SRK EoS: $k_{ij} = -0.0001 \cdot T + 0.1233$ (7)

$h_{ij} = -0.0001 \cdot T + 0.0083$ (8)

PR EoS: $k_{ij} = -0.0002 \cdot T + 0.1514$ (9)

$h_{ij} = -0.0003 \cdot T + 0.0467$ (10)

From Table 2 it can be observed that the interaction parameter k_{ij} is quite large, indicating strong interactions between the small polar molecules of CHF_3 and large molecules of 1-phenylpropane.^{20, 21} The temperature dependence of both interaction parameters is given by the equations (7-10) and is plotted in Fig 6.

It can be observed that for the studied temperatures range, the parameters are not very temperature dependent. This is also confirmed by the small values of the slope in the equations (7–10).

CONCLUSIONS

LV, LL, LLV equilibrium data for the system consisting of CHF_3 +1-phenylpropane were measured for temperatures range of $T=250 - 400$ K and pressures up to 15 MPa. According to the general classification of van Konynenburg and Scott, the system develops type III phase behavior. The coordinates of the UCEP reported in this work does not have correspondence in the literature, so far.

Modelling VLE data with PR and SRK EoSs and van der Waals mixing rules show good fit with $AADP < 2.5$, except the critical region. The use of two parameters in the mixing rules leads to a better description of the phase boundaries compared with 1PCMR. The parameters in the mixing rules were optimized and correlated with temperature and components interaction.

Comparison with the experimental data recommends calculations with SRK/2PCMR for temperatures below the UCEP, while for temperatures above the UCEP, PR/2PCMR gives better results.

The model based on PR/SRK EoSs coupled with conventional mixing rules prove to be a useful tool to predict the LV equilibrium in the asymmetric system consisting of HFC, refrigerant and alkylbenzene.

REFERENCES

1. M.Youbi-Idrissi and J. Bojour, *Int. J. Refrig.*, **2008**, *31*, 165-179.
2. A. Yokozeki, *Int. J. of Thermophys.*, **2001**, *22*, 1057-1071.
3. N. Elvassore and A. Bertucco, *Ind. Eng. Chem. Res.*, **1999**, *38*, 2110-2118.
4. J.S. Fleming and Y.Yan, *Int. J. Refrig.*, **2003**, *26*, 266-274.
5. R. Tesser, M.Di Serio, R. Gargiulo, G.Basile, L. Bragante and E.Santacesaria, *J. Fluor. Chem.*, **2003**, *121*, 15-22.
6. K.N. Marsh and M.E. Kandil, *Fluid Phase Equil.*, **2002**, *199*, 319-334.
7. K. Takigawa, S.I. Sandler and A. Yokozeki, *Int. J. Refrig.*, **2002**, *25*, 1014-1019.
8. E.D. Nikitin, A.P. Popov and N.S. Bogatishcheva, *J. Chem. Eng. Data*, **2002**, *47*, 1012-1016.
9. R.C. Reid, J.M. Prausnitz and B.Poling, "Properties of Gases & Liquids, McGraw-Hill Book Company, Singapore, 1988, 4th Edition, p. 670-718.
10. Th.W. de Loos, H.J. van der Kooi and P.L.Ott, *J. Chem. Eng. Data*, **1986**, *34*, 166-171.
11. K. Ohgaki, S. Umezono and T. Katayama, *J. Supercrit. Fluids*, **1990**, *3*, 7825-7829.
12. Th.W. de Loos and W. Poot, *Phys. Chem. Chem. Phys.*, **1999**, *1*, 4293-4297.
13. J. M Prausnitz, R. N. Lichtenhaler and E.G. de Azevedo, "Molecular Thermodynamics of Fluid Phase Equilibria", Prentice Hall Inc., Toronto 1986, 2nd Edition, p.443-453.
14. W. Poot and Th.W. de Loos Fluid Phase Equilibria, **2004**, *222-223*, 255 -259.
15. C. Bogatu, R.Vilcu, A. Duta and Th.W. de Loos, 17th International Congress of Chemical and Process Engineering, CHISA 2006, CD proceedings, ISBN 80-86059-40-5, 27-31 August, Czech Republic.
16. S. E. Quinones-Cisneros, *Fluid Phase Equilib.*, **1997**, *134*, 103-112.
17. Wei, Y. S. and Sadus, R. J., *AIChE J.*, **2000**, *46*, 169-196.
18. D.Geana and V. Feroiu, "Ecuatii de stare – Aplicații la echilibre de faze", Ed. Tehnică, București, 2000, p. 91-150.
19. A.Duta, "Proprietăți PVT și echilibre lichid-vapori în sisteme de n-alcani", PhD Thesis, București, 1997.
20. L. Calvo and Th.W.de Loos, *Fluid Phase Equilib.*, **2006**, *244*, 179-187.
21. V.V.de Leeuw, W. Poot, Th.W.de Loos and J.de Swaan Arons, *J. Chem. Eng. Data*, **1994**, *39*, 143-146.